This is the author's version (manuscript) of the work that was accepted for publication in Journal of Spacecraft and Rockets.
The Version of Record is available online at https://doi.org/10.2514/1.A35252

Thermal investigation of a purged insulation system for a reusable cryogenic tank

Thomas Reimer *, Carolin Rauh † and Giuseppe D. Di Martino ‡
German Aerospace Center (DLR), 70569 Stuttgart, Germany

Martin Sippel §
German Aerospace Center (DLR), 28359 Bremen, Germany

To advance reusable space transportation vehicles with cryogenic tanks for future space missions, a reliable thermal management system must be developed. To do so, the challenge of insulating the propellant while in the same time protecting the structure against re-entry heat loads needs to be addressed. A possible insulation design including a structural fixation element for the thermal protection system was developed as part of the DLR-project AKIRA. As key feature a purged gap was implemented between cryogenic and high-temperature insulation to reduce overall layer thickness. Thermal experiments simulating both steady-state refueling phase and transient re-entry phase proved that the defined thermal boundary conditions of the reference configuration could be met. The insulation system design is outlined in brief and both the experimental setup and the test results are presented and discussed.

I. Introduction

Reusable launch vehicles (RLV) present the opportunity to reduce space mission costs significantly, but the challenges of developing reliable and low-maintenance transport systems are many-faceted. One of them concerns the design for reusable propellant tanks of space vehicles in the case when cryogenic liquid fuels are used. On the one hand, the vehicle requires a thermal protection system (TPS) for performing the re-entry unscathed, which consists of a highly porous high-temperature (HT) insulation and a surface panel. However, as a governing requirement for the TPS sizing, it was defined that during the pre-launch tank refueling phase, temperatures must remain positive within the HT-insulation to prevent frost accumulation due to condensation and freezing of humid air which could lower the insulation performance significantly, as suggested in [1] and [2]. This, on the other hand, leads to specific issues with the sizing of a purely thermal insulation of the tank with regard to the design of the TPS. The design problem is to find a good compromise between proper low-temperature insulation performance considering also boil-off rates during the

*Research Scientist, Dep. Space Systems Integration, Institute of Structures and Design, Pfaffenwaldring 38-40, 70569 Stuttgart
†Research Scientist, Dep. Space Systems Integration, Institute of Structures and Design, Pfaffenwaldring 38-40, 70569 Stuttgart
‡Ph. D., Research Scientist, Dep. Space Systems Integration, Institute of Structures and Design, Pfaffenwaldring 38-40, 70569 Stuttgart, AIAA Member Grade
§Ph. D., Head of Department Space Launcher System Analysis, Institute of Space Systems, Robert-Hooke-Str. 7, 28359 Bremen, AIAA Member Grade

pre-flight tank filling, sizing of the TPS for re-entry including consideration of fixations as possible thermal shorts, and weight optimization.

The integration of a cryogenic insulation and a TPS onto an RLV tank structure was one of three selected key issues of RLV development to be addressed in detail with the multidisciplinary research project AKIRA of the German Aerospace Center (DLR) [3]. To meet the thermal requirements while saving weight, an attachment system including a purge gap was realized to thermally decouple the cryogenic insulation on the tank wall from the TPS insulation on the outside of the vehicle. In the following, the system development process is outlined together with the corresponding experimental setup and the test results are presented and discussed.

II. System Design

A. Insulation system sizing

The winged booster stage of the SpaceLiner7 concept (SL7) [4] was used as reference configuration for the investigations. As depicted in Fig. 1b) and c), the booster consists of integral cryogenic aluminum tanks for liquid oxygen (LOX) and liquid hydrogen (LH2). It shall be jettisoned at about Mach 12 and is supposed to land horizontally. The corresponding time-dependent re-entry heat flux densities for selected design points on the booster exterior wall near the tanks are shown in Fig. 1a). According to this, the highest heat loads are expected at the windward side of the oxygen tank (P1) with values up to 78kW/m^2, which were determining for the following TPS design and the subsequent experimental procedure. For the overall insulation system design, including both the TPS with the HT-insulation and a possible separate cryogenic insulation, two different thermal load cases were considered:

- pre-flight steady-state condition with fully loaded tanks on the launch pad.
- transient thermal load profile during ascent and re-entry.

To size the required insulation thickness, thermal numerical simulations were done using a one-dimensional FEA model. The numerical tool of choice was the ANSYS® Workbench environment [5]. Initial considerations made it clear that it is not possible to just utilize the TPS without any other underlying dedicated insulation of a different type. This is due to the fact that the open-pore HT-insulation shall be kept at temperatures above freezing point to prevent internal frost build-up. In the steady-state condition on the launch pad, the tank structure cools down to the fuel temperature, which means that in any insulation that is situated directly on the tank wall there will be a very low temperature. Therefore, it was decided to investigate a system of two insulation layers, with a dedicated cryogenic insulation directly at the tank wall and a HT-insulation as part of the TPS on top.

As cryogenic insulation, the polymethacrylimide-based closed-cell rigid foam Rohacell® [7] was chosen and the HT-insulation consisted of the open-pore alumina silica fiber insulation ALTRA® Mat [8]. Consequentially, two thermal requirements (R1, R2) were set up as design criteria which had to be met during the following thermal numerical

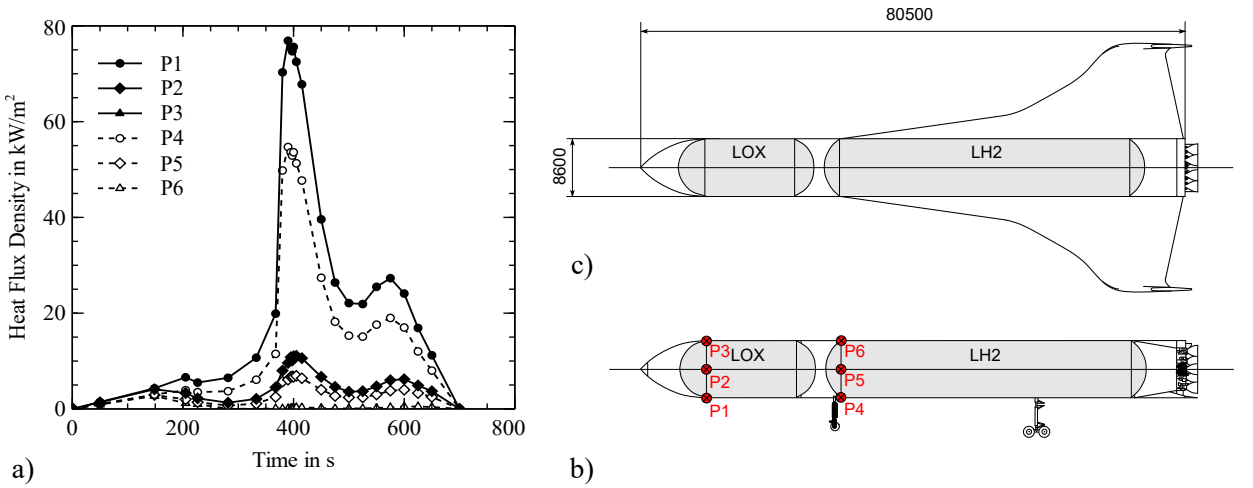

Fig. 1 a) Transient thermal re-entry heat loads for selected design points on the SL7 booster shown in b). b) Schematic SL7 booster layout side view and c) topview. [6]

simulations. The first defines that the HT-insulation in the TPS shall be above zero degree Celsius to prevent internal frost build-up, the second defines that the interface temperature between HT-insulation and the underlying cryogenic insulation shall be below 100°C to prevent it from deteriorating.

R1: Minimum temperature of 0°C for the TPS during tank refueling.

R2: Maximum temperature of 100°C for cryogenic insulation during booster re-entry.

The numerical simulations were done in a sequential way, with the steady-state simulation first, followed by the transient simulation of ascent and re-entry, using the result of the steady-state case as the input condition for the transient case. The results showed that a combined insulation system of 105 mm of Rohacell and 13 mm (LH2 tank) and 15 mm thickness (LOX tank) of HT-insulation meets both requirements.

Table 1 Thickness result of the combined TPS and cryogenic insulation system without purge gap.

Design Point	Tank	Cryo insulation, mm	TPS insulation, mm	Total thickness, mm
P1	LOX	105	16	121
P4	LH2	105	13	118

The resulting total insulation thickness of 118 mm and 121 mm was considered to be quite large and it was discussed if there was a way to reduce the total thickness. As a result it was decided to introduce a dedicated purge gap into the system between the two insulation layers, through which dry gas shall be fed during the steady-state tank fueling phase, as shown schematically in Fig. 2a). Consequently, condensation is prevented by two basic mechanisms: firstly, thermal energy is transported into the system and secondly, moist air is impeded from intruding into the TPS. The purge gap system can be regarded as element of active thermal management of the whole system. Via selecting the parameters of the purging system, as there are gas temperature, gas velocity, gap width etc., a wide range of conditions can be achieved.

The drawback of the system is that a considerable amount of thermal energy is fed into the system, which predominantly goes towards the direction of low temperature, i.e. towards the cold tank , and is heating up the fuel, so there will be an increased rate of fuel boil-off while on the ground. However, thermal analyses proved that a considerable thickness reduction by 45% compared to a non-purged system based on the selected flow parameters can be achieved [9].

Finally, due to the expected low heat load and easier handling, it was decided that the surface panel was made of Inconel600. As a consequence of the results of the thermal simulations, it was pre-oxidized to achieve the required reflection properties to dissipate re-entry heat fluxes.

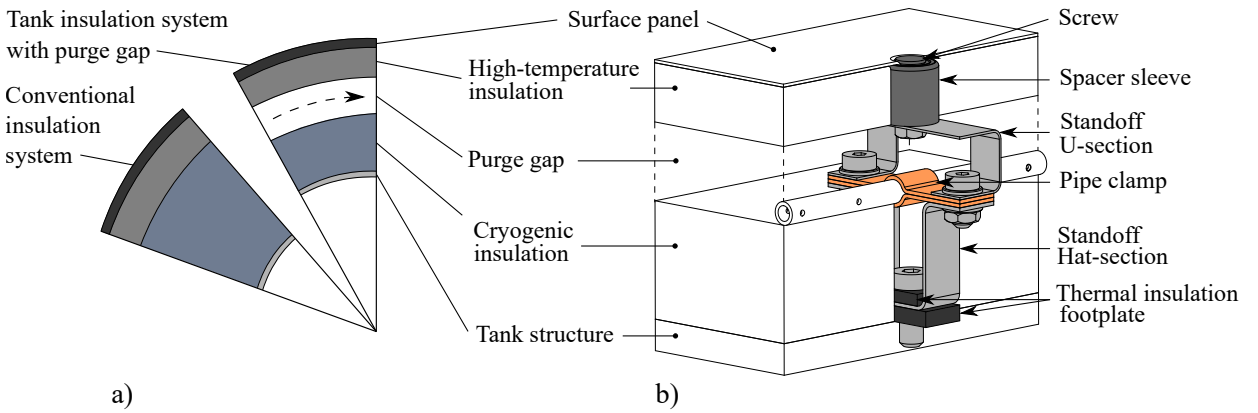

Fig. 2 a) Tank insulation system comparison unpurged and purged. b) Section of the ITO including standoff and gas pipe.

B. Purge system and TPS interface design

The considerations on the purge system outlined above were based on very basic estimations of the relevant gas parameters without taking into account the actual hardware items that are required to build such a system on a vehicle. However, since the AKIRA project required to build an integrated test object to verify the proposed systems, different designs to realize a purging system were discussed. As for the actual purge gap, a spacer mesh fabric of 20 mm thickness of high permeability and little flow resistance to the purge gas was introduced [10]. The stack of mesh spacer fabric and HT-insulation is held in place by the rigid surface panels which are mechanically attached to the tank structure. For what concerns the gas feed system, it was decided to choose a design based on a grid network of tubing. The tubes feature small boreholes in regular intervals out of which the gas flows into the purge gap. The detailed question of where the gas exits the whole system was excluded from the considerations for the moment. It is assumed that the overall system can be designed in such a way that the gas flow can be collected on the leeside of the vehicle to exit there into the environment.

To attach the surface panels and to hold the tubing system, a fixation structure had to be developed. From the thermal simulations of the ideal situation of the layered insulation it was obvious that any additional structural element with higher thermal conductivity between hot surface panel and cold tank structure would act as a disturbance to the

temperature field, creating a thermal short of some sort with temperatures being too low during steady-state because of the good thermal contact to the tank structure. Therefore, the idea was to make use of the need for fixation points for the gas feed tubes and integrate them into the fixation points of the TPS, thereby achieving the possibility to control also the temperature of the fasteners at the purge gap interface using the convective heating of the purge tubes.

The resultant concept for a structural standoff is shown in Fig. 2b). As a key feature, the standoff was divided into multiple parts of different thermal conductivity to minimize the thermal bridge effect. In addition, an isolating footplate below the undermost part of the standoff reduced the required amount of heating from the purge tube to meet R1. To facilitate a good thermal contact between the purge tube and the standoff, the tube was brazed into a set of two thin strips of copper alloy which were clamped between the upper and lower elements of the standoff assembly, thereby effectively separating the hot and the cold side by providing thermal energy to flow into the cold parts. Finally, the standoff parts exposed to high thermal loads during re-entry were made of Inconel600 like the surface panel, while the remaining components were made of stainless steel. Furthermore, the standoff was designed to compensate the thermal expansion mismatch between hot surface components and the cryogenic tank structure by elastic deformation.

The U-section of the standoff is supposed to be riveted to both the pipe clamp and the hat-section and the connection between surface panel and standoff is suggested to be made with a pin. In this case, a wave spring would additionally support the panel to be independent from the HT-insulation stiffness. However, bolted joints were used for the experimental investigation to have the possibility of non-destructive disassembly for visual inspection.

The insulation design process was supported by computational fluid simulations done with ANSYS CFX [11]. The goal of the parameter study was to find an order of magnitude for both the purge gas temperature and the mass flow needed to keep the HT-insulation above 0°C without simultaneously putting more heat energy into the tank than necessary. As an additional requirement, the maximum flow velocity inside the pipe was limited to subsonic values. The results indicated that a purge mass flow of approximately 2.0g/s and gas temperatures of 15°C could satisfy the defined requirements. A detailed description of the fluid simulations and the results can be found in [12].

III. Experimental setup

To verify the thermal efficacy of the purge gap concept, an integrated test object (ITO) was built to be tested in the DLR thermo-mechanical test facility INDUTHERM. The ITO, depicted in Fig. 3, was a representative 400x400mm section of the above-described tank insulation design. As the objective was to investigate the thermal processes without any mechanical testing, a single central standoff carrying one purge gas pipe was included, as depicted earlier in Fig. 2b).

The purge gas entered the purge gap from the pipe through small holes of 1.5mm diameter spaced 20mm apart. Each standoff component and each layer interface was instrumented at defined locations with sheathed type-K thermocouples of 0.5mm diameter. In addition, thermocouples were attached in four locations each on the interfaces of purge gap and cryogenic insulation and HT-insulation, respectively. They were located 100mm from the pipe and 65mm from the ITO

center line perpendicular to the pipe to determine the temperature field in the purge gap at a distance from the purge tube. Furthermore, the purge gas temperature was monitored with Pt100 sensors located at the ITO pipe inlet and outlet. Purge gas inlet and outlet total pressure were measured by pressure gauges of the P33X-series (Keller AG) with a range of 0-300bar. Mass flow was measured and controlled with the digital mass flow controller MASS-STREAM D-6370-DR.

To heat the purge gas for which gaseous nitrogen was used, the gas feed line was routed through a temperature controlled water bath. The temperature was controlled by an ETC4420-230 PID temperature controller and the water temperature was monitored by a type-K thermocouple. To enhance the heat transfer to the gas, the pipe segment inside the water was made of copper alloy. From the water bath to the ITO the gas feed line was made of an insulated flexible plastic hose to keep the gas temperature as constant as possible.

In the INDUTHERM test chamber, the ITO was placed with the aluminum plate facing up, as depicted in Fig. 4. Surrounding insulation plates placed between ITO and chamber walls and the aluminum plate of the ITO formed a basin, lined with PTFE foil, into which liquid nitrogen (LN2) was filled as propellant substitute. While providing the basin walls, the insulation plates additionally insulated the sides of the ITO from thermal convection, thus preventing edge effects distorting the measurements.

An inductively heated, 200x200mm graphite susceptor plate located in a cavity underneath the surface panel provided the heat source to simulate the re-entry heat load. To avoid buckling caused by localized heating, the metallic surface panel was designed with a square circumferential expansion gap. The resulting inner panel had the same area like the susceptor plate.

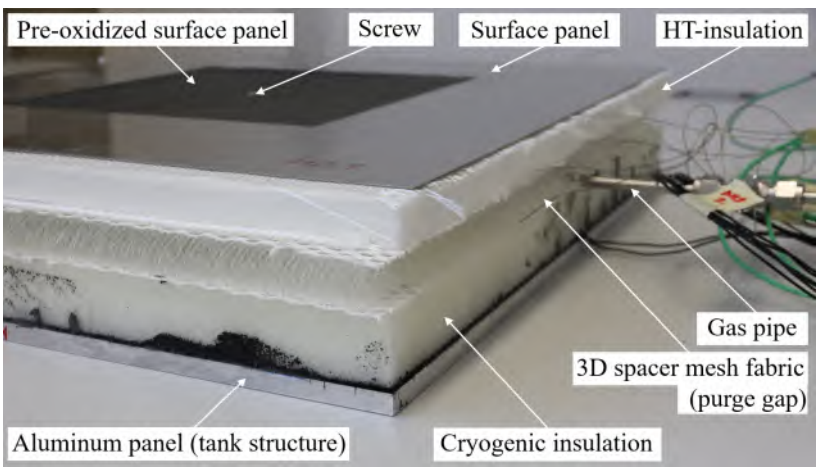

Fig. 3 Fully assembled ITO.

A. Testing procedure

During the steady-state tests in ambient atmosphere, the ITO was purged with the constant inlet gas mass flow $\dot{m}_{In}$ and the gas temperature T_{In}, while the basin was constantly refilled with LN2. An overview of the flow conditions of the

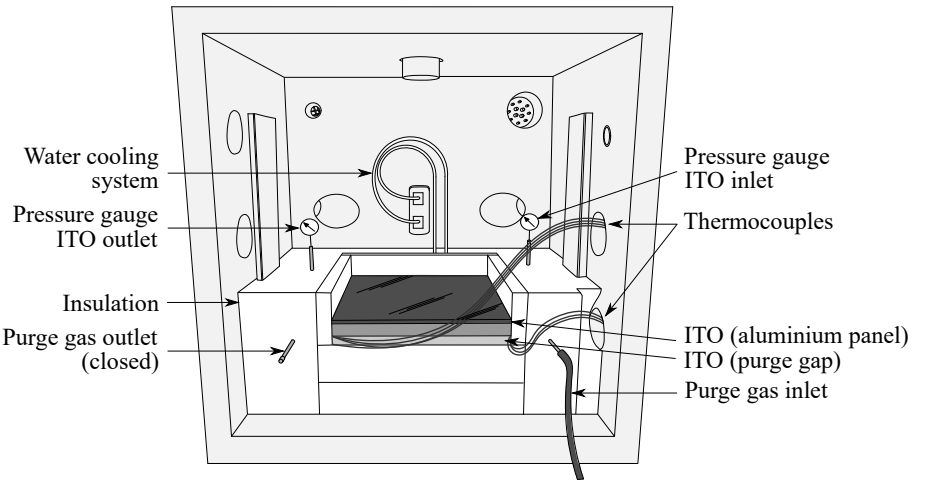

Fig. 4 Illustration of the INDUTHERM test setup (steady-state phase) with removed front insulation panel.

14 steady-state test runs carried out is given in Table 2. A test run was considered completed after all thermal signals reached steady-state with no significant changes.

Table 2 Experimental conditions of the purge flow during the steady-state tests in ambient atmosphere.

Test-ID	Gas inlet temperature T_{In}, °C	Mass flow $\dot{m}_{In}$, $\frac{g}{s}$	Test-ID	Gas inlet temperature T_{In}, °C	Mass flow $\dot{m}_{In}$, $\frac{g}{s}$
St1	17	2.5	St8	24	2.5
St2	21	1.5	St9	32	1.5
St3	21	2.0	St10	32	2.0
St4	21	2.5	St11	32	2.5
St5	24	1.0	St12	38	1.5
St6	24	1.5	St13	38	2.0
St7	24	2.0	St14	38	2.5

For the transient test runs, the same procedure was performed to cool down the ITO in the first place, as the vehicle tank structure is supposed to be still cold when entering the re-entry phase of the flight. As a consequence of the results of the preceding steady-state test runs, the flow parameters T_{In} and $\dot{m}_{In}$ of both St11 and St13 were used for purging. After the thermal steady-state was reached, the purging was stopped and the test chamber was closed after the LN2 had evaporated completely. Subsequently, the chamber pressure was reduced to approximately $p_{min} < 1$mbar and the heating procedure started. Preliminary testing was carried out to work out the optimum inductive heating cycle for the susceptor to achieve the calculated time-dependent re-entry heat load for design point P1 on the ITO surface panel. However, the maximum heating power was gradually reduced with the next test runs as the maximum temperatures in the ITO exceeded the simulated maximum values in the first place. A transient test run was considered completed after

all temperatures decreased again after they passed their maximum. When the susceptor temperatures dropped below 400°C, the chamber pressure was raised again and the preparations for the next test run could be started.

An overview of the experimental conditions of the transient test runs including the purge flow conditions used for the precedent simulated tank filling phase is given in Table 3. Note that the first test run Tr1 was aimed purely at obtaining a temperature step profile for validating the numerical model. In order to achieve that, the susceptor was heated rapidly to 500°C and the temperature was maintained for 5 minutes.

Table 3 Experimental conditions of the transient test runs.

Test-ID	T_{In}, °C	$\dot{m}_{In}$, $\frac{g}{s}$	$T_{max,susceptor}$, °C	p_{min}, mbar
Tr1	38	2.0	502.7	0.5
Tr2	31	2.5	943.4	0.8
Tr3	38	2.0	885.7	0.5
Tr4	38	2.0	808.0	0.4
Tr4-rep	38	2.0	805.8	0.2

IV. Results

A. Steady-state tests

The objective of the steady-state tests was to find a flow parameter combination with the lowest possible T_{In} and $\dot{m}_{In}$ which nevertheless reliably prevents temperatures below 0°C in the HT-insulation. This requirement was considered satisfied if all thermal sensors located inside the HT-insulation and at the interface to the purge gap recorded positive temperatures as steady state. With the testing procedure described above, the usual time to achieve steady state was 30-50 minutes. The positions of the thermal sensors at the standoff are marked in Fig. 5a), with the standoff depicted upside down with the aluminum plate facing up like it was mounted in the experimental setup. The locations of the purge gap interface thermal sensors are marked in Fig. 5b), showing the topview of the purge gap, with the P-Cryo-sensors and the P-HT-sensors facing each other directly.

The resultant final temperatures of the standoff thermal sensors for the test runs St1 to St14 are shown in Fig. 6a) grouped by purge gas inlet temperature T_{In} for increasing mass flow rate and grouped by inlet mass flow rate for increasing T_{In} in Fig. 6 b). Due to their positions close to or directly on the aluminum panel which was in direct contact with the LN2, the temperature signals at S01, L01 and S02 were always significantly below -100°C. Hence, their signals are not included in the graphs as they did not show any significant differences between the test runs. Therefore, the critical thermal signals to be looked at in this case are S06 which was attached to the stainless steel U-section of the standoff near the HT-insulation, and S07 located within the HT-insulation with contact to the screw. Looking at the data for each test, it is evident that a thermal gradient formed from the aluminum panel to the surface panel on the other side.

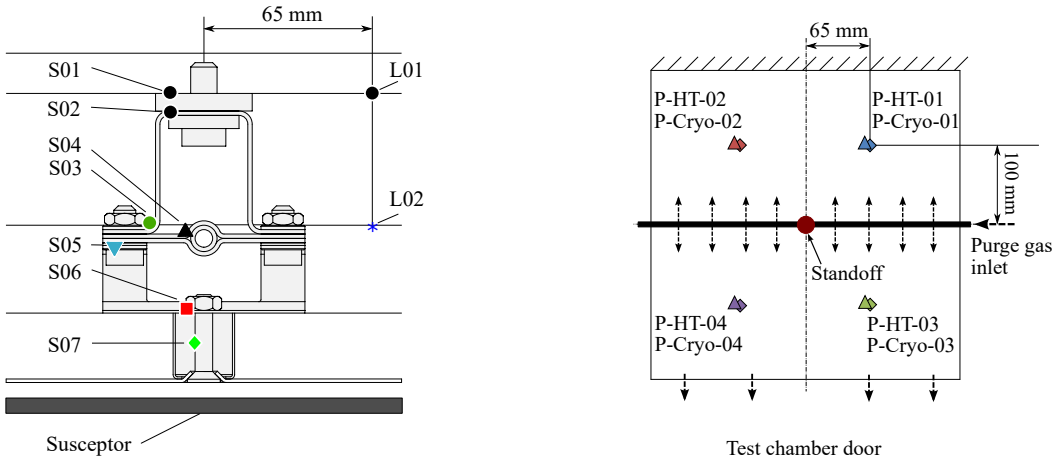

Fig. 5 Thermal sensor locations at the standoff (a) and in-plane at the purge gap interfaces (b).

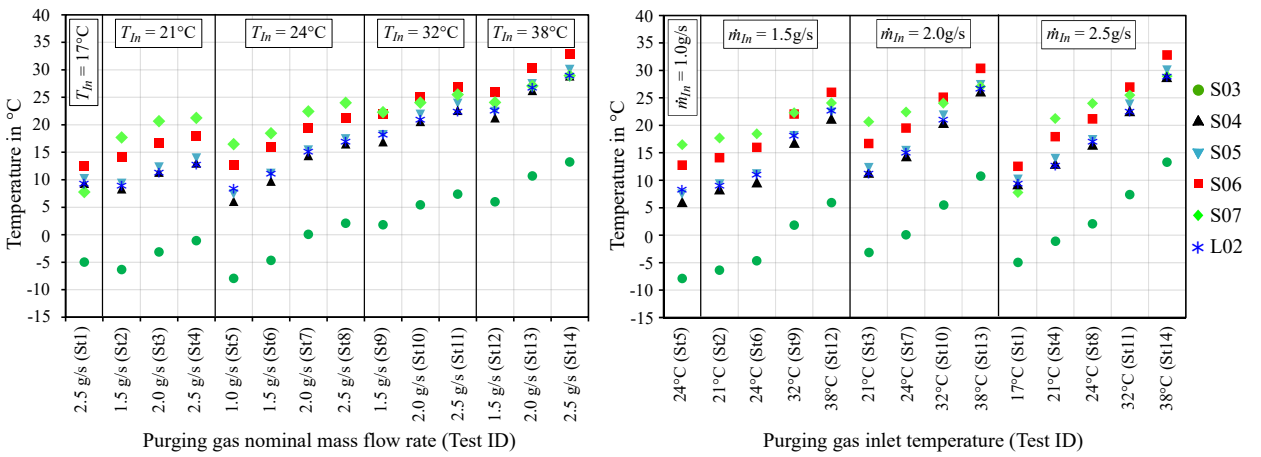

Fig. 6 Resulting steady-state standoff temperatures of the test runs St1 to St14.

Nevertheless, the copper pipe clamp prevented the diffusion of low temperatures into the TPS through the standoff materials remarkably well, with an average temperature difference of 20°C between S03 and S06.

If the results are also grouped by inlet mass flow, as shown in Fig. 6b), it is clear to see that the signal at S03 usually reached or even exceeded 0°C for inlet mass flow rates of $\dot{m}_{In}$ = 2.5g/s and for inlet gas temperatures of $T_{In} \geqq 32$°C. The temperatures were even higher at L02, which monitored the interface temperature of the spacer fabric and the cryogenic insulation at a distance of 65mm from the pipe, centered on the ITO (200mm downstream from the gas inlet), with 8°C the lowest (St5) and 29°C the highest values (St14) recorded at this location.

The in-plane temperatures of the purge gap interfaces to the cryogenic insulation and the HT-insulation are shown in Fig. 7a) grouped by inlet temperatures and in b) grouped by inlet mass flow rate. In both graphs, the hash marks are for

the steady-state temperatures on the cryogenic insulation (P-Cryo) and the triangles represent the temperatures on the HT-insulation (P-HT).

For the tests performed with T_{In} = 32°C and 38°C, some of the temperatures at the HT-insulation interface to the gap (P-Altra-03, P-Altra-04 and S06) show higher temperatures than at S07 inside the HT-insulation because the gas temperature exceeded the ambient temperature considerably, which was usually around 21°C. Looking at the data relative to the thermal signals P-Cryo and P-Altra, it is evident that also a planar thermal gradient formed within the gap, with higher temperature in the fore side, where the opening in the insulations surrounding the ITO let the purging flow go out easily, and lower temperature in the back side, where recirculation regions are assumed to have formed.

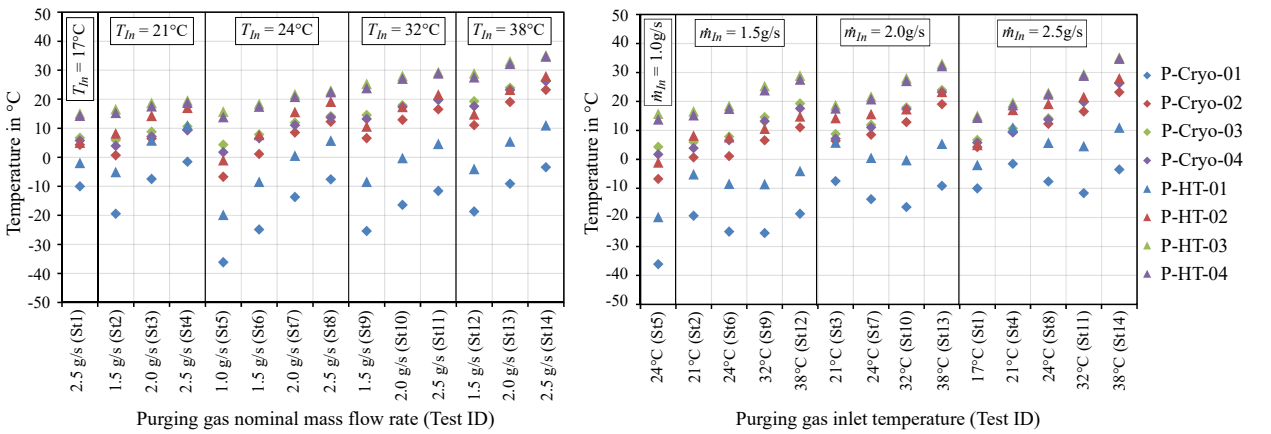

a) **b)**

Fig. 7 Resulting steady-state interface temperatures of the test runs St1 to St14.

Comparing the experimental results of the different tests, a general increase of the temperature by both increasing the purge gas mass flow rate and the purge gas inlet temperature can be observed, as it was expected. However, the resulting temperatures at P-Cryo-01, P-Cryo-02, P-HT-01 and P-HT-02 (in the gap on the back side of the ITO) do not show a clear behavior. To verify the repeatability and to further investigate the thermal behavior of the sensors on these locations, both test runs St2 and St6 were repeated. The results of the repeated test runs showed good agreement to the first runs, except for the mentioned in-plane thermal signals L02, P-Cryo-01 and 02 and their facing equivalents on the HT-insulation, P-HT-01 and 02, which differed by between 0.3°C and 9.3°C. Nevertheless, the average difference of all temperatures of the repeated test runs St2-rep and St6-rep was 0.6°C and 3.4°C, respectively. This order of magnitude was later confirmed by the precedent cooling phase of the transient test runs, for which St11 and St13 were repeated.

The deviation and the irregular behavior of the in-plane temperature signals were finally assumed to be the effect of flow vortices occurring in the back of the purge gap, as the only exit for the flow was to the front out of the test chamber. The inevitable presence of gaps between the ITO and the insulation in the test chamber also could have caused undesired convective phenomena disturbing the temperature measurements in the gap.

Finally, the mean steady-state temperature and pressure differences between the gas pipe inlet and outlet were evaluated. The percentage change of temperature and pressure occurring along the pipe length of 400mm for the test runs St2 to St14 are shown in Fig. 8. It is clear to see that with increasing mass flow rate the temperature drop decreased while the pressure drop increased. This correlation is best observed by looking at St5 with the minimum test inlet mass flow of $\dot{m}_{In}$ = 1.0g/s, leading to the highest measured temperature drop with 50% and the lowest pressure loss of 9% of all test runs. In the contrary, the lowest temperature decrease and the highest pressure drop occurred during St11 with only 4.1% compared to T_{In} and 33% compared to p_{In}. However, concerning the pressure decrease it needs to be taken into account that the pipe outlet was sealed for the experiments to force the purge flow through the holes into the gap.

To ensure the best starting conditions for the transient test runs, the flow parameters of St11 ($\dot{m}_{In}$ = 2.5g/s and T_{In} = 32°C) and St13 ($\dot{m}_{In}$ = 2.0g/s and T_{In} = 38°C) were chosen for simulating the tank-filling and ascent phase.

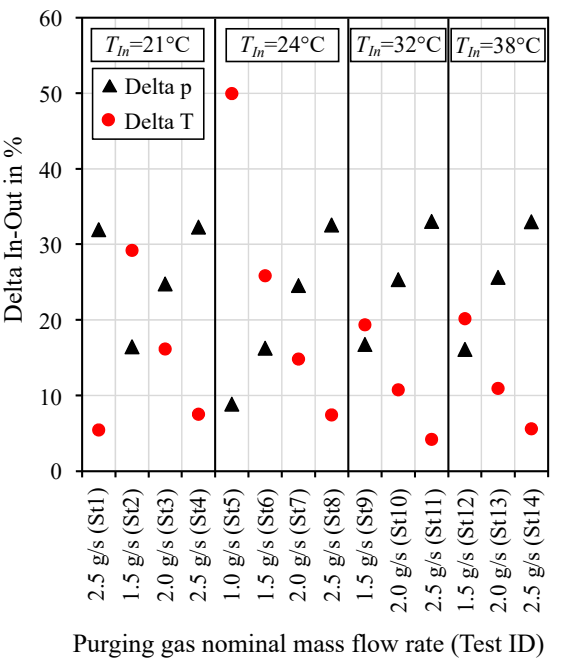

Fig. 8 Percentage change of inlet temperature and inlet pressure along the pipe length grouped by gas inlet temperature.

B. Transient tests

The main objective of the transient tests was to show that the maximum temperature within the cryogenic insulation did not exceed 100°C during the re-entry phase of the flight. This criterion was set conservatively, as the manufacturer of the material specifies a maximum application temperature of 130°C and even 180°C, which can be tolerated for a limited time. Therefore, the critical measuring points for this criterion were the ones located on the surface of the cryogenic insulation P-Cryo-01 to -04, L02 and S03, which was attached to the standoff near the insulation. The resulting temperature profiles within the ITO as well as the susceptor temperature profile and the chamber pressure for

one representative test run (Tr4) are presented in Fig. 9. The graph starts just before the inductive heating phase, hence the temperature profiles of the previous purged LN2-cooling phase is not shown. The graphite susceptor was heated rapidly to about 800°C within 340 seconds, and it can be seen that the thermal signal of S07 followed the increasing temperature almost instantly. After the required maximum temperature of the susceptor was reached, the inductive heating power was switched off and the susceptor cooled down gradually as a result of radiative and conductive heat transfer to the surrounding components. With 76 seconds delay after the susceptor maximum temperature, the ITO maximum temperature was reached at S07 with 629°C. However, the other thermal signals reached considerably lower maximum temperatures with greater delay. The P-Cryo sensors measured 95°C as the highest temperature, which is below the acceptable maximum temperature.

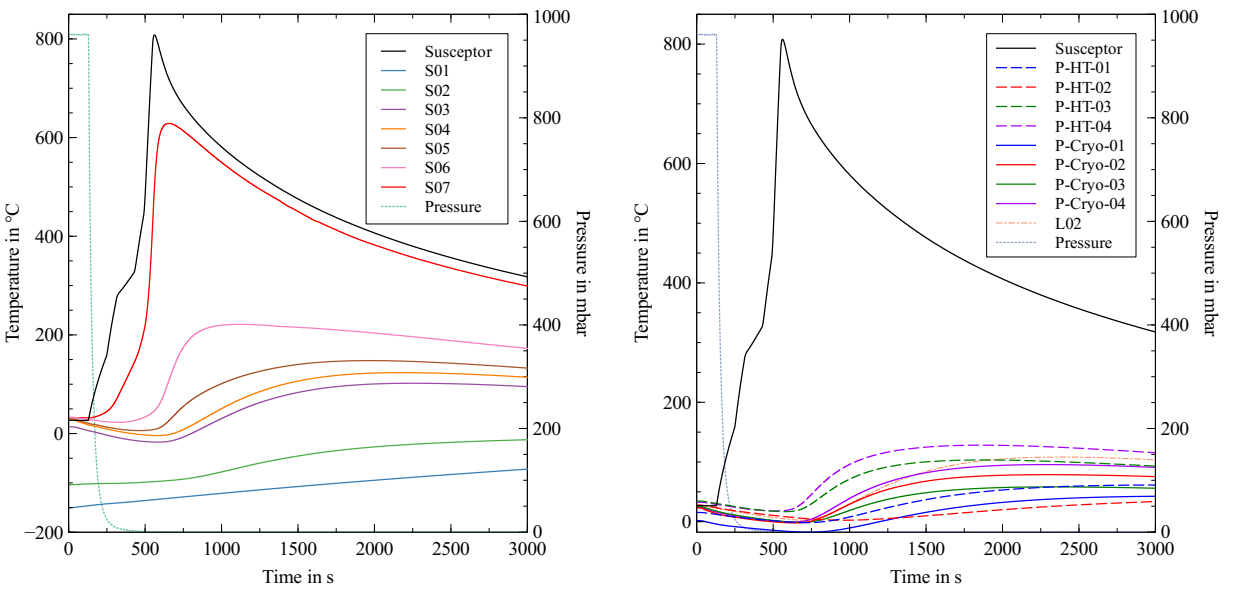

Fig. 9 Transient temperature profiles of the standoff thermal sensors (a) and the in-plane interface thermal sensors (b) of test run Tr4.

In contrast to the booster re-entry heat load presented in section II.A, only the first temperature peak could be simulated properly, due to the lack of convective cooling within the vacuum chamber after switching off the heating power. As a further consequence, the integral heat load acting on the surface panel of the ITO was significantly larger than the heat load which is assumed for the booster exterior wall. To quantify the effect, the simulation results for both the surface panel temperature and the temperature at the thermocouple position S07 resulting from the calculated heat load for the booster exterior wall and the the experimental temperature profile at S07 were compared and are shown in Fig. 10. It can be seen that the experimental curve fits the reference curve very well up to the maximum temperature after 500 seconds, although it exceeded the simulated maximum temperature for S07 by 63°C or 11%. Despite the

higher temperature load, the critical thermal sensors reached only 95% of their allowed maximum temperature during the experiments, which shows that the insulation system fully complied to the requirement R2.

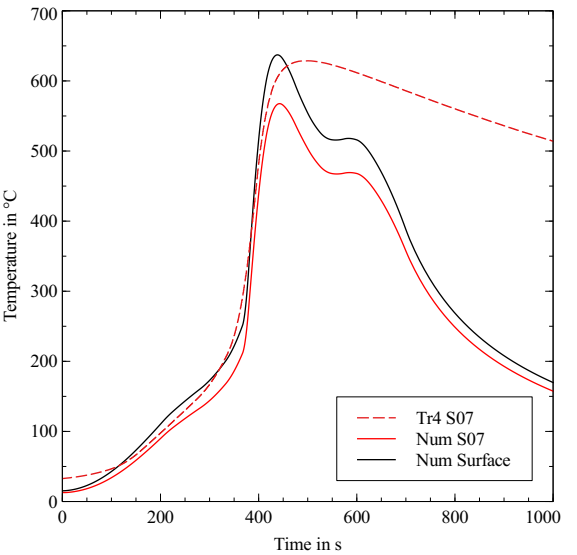

Fig. 10 Comparison of simulated and measured temperatures at the ITO surface and S07.

V. Discussion

The results of the steady-state tests show that by choosing suitable parameters for the purge gas flow, as there are gas temperature and mass flow rate, conditions in the HT-insulation can be achieved which comply to the requirement R1, calling for a temperature always higher than zero degree Celsius to prevent internal frost build-up. As shown in the figures 6a) and b), both parameters, gas temperature and mass flow rate can be used independently to achieve the desired effect, giving a great deal of variability to the system design. Regarding the test results of steady-state test St8 and later, the temperatures in the HT-insulation were significantly higher than 0 degree Celsius when the measurement position P-HT-01 is discarded because it reflects a specific condition of the test item being not representative. In those cases where the mass flow rate was equal to or higher than 2.0 g/s, with gas entry temperatures 32 degree Celsius or higher, the temperatures in the HT-insulation were in the range of between 20 to 30 degree Celsius. These conditions for the purging gas can be easily achieved and supplied to the purging system which is an important finding with regard to application in a possible future demonstration vehicle.

Another important aspect was the control of the interface temperatures at the structural connections between the surface panel and the tank since there is a path of increased thermal conductivity compared to the insulation materials. The results of both steady-state and transient tests showed that the temperatures at these interfaces can be controlled effectively. In the case of steady-state conditions, the direct connection of the heated purge gas feeding tube to the standoff effectively kept the temperature of the standoff part inside the HT-insulation at temperature levels close to that

of the gas entry temperature. In Fig. 6 it is obvious that the measurement locations S04 to S07 are distinctly separated in temperature from those of S03 (S01 and S02 not shown because of much lower temperatures).

In the case of the transient re-entry conditions, the higher conductivity of the standoff components was in fact of advantage to compensate for the increased heat flow coming from the surface panel as a result of the simulated re-entry heat load. Due to the fact that the purge flow was stopped at the end of the steady-state tests, the thermal short between cold tank and surface panel was re-established as can be seen by the initial temperature drop of the standoff temperatures in Fig. 9. Therefore, the incoming heat from the surface panel could be conducted to the cold tank structure without pushing the standoff temperatures in the cryogenic insulation above the material limit value of 100°C, which had been defined by the requirement R2.

Since the investigations were done on a test article of limited size, there is a need for further investigations with regard to the size effects that are to be expected when an operational vehicle is anticipated with tube lengths of several meters. In that case, the longer purge lines will lead to a higher pressure decrease with increasing distance from the inlet and resulting lower mass flow rates towards the far end of the purge tube. This effect could be compensated via increasing the sizes of the purge gas exit orifices in the purge tube with the distance from the gas inlet. In addition, the diameter of the purge tube could be variable over its length. Another option could be to include parallel purge gas feed lines without exit orifices to intermediate stations to have again the high inlet pressure value.

Another issue which should be investigated in more detail is the question if the HT-insulation has to be kept at temperature values greater than zero degree Celsius at all times, because this requirement R1 was in fact the driving issue for adding quite some complexity in terms of the purging system. There is some literature suggesting this as a guideline [13–15], however, no quantification of the possible adverse effects could be found if the temperature is in fact allowed to decrease under zero degree Celsius. It would be interesting to investigate the effects of the internal frost build-up in terms of mass increase and on the insulation performance in a dedicated test program when specific temperature levels and certain exposure times are selected.

VI. Conclusion

An insulation system design comprising a cryogenic insulation, a thermal protection system and a fixation element was developed for a reusable cryogenic booster stage as part of the DLR-project AKIRA. Two design-determining thermal requirements were derived from the reference configuration of the SpaceLiner7-booster stage. First, the minimum temperature for the high-temperature insulation was set to 0°C during the pre-flight steady-state condition, when the tank is fully loaded on the launch pad, to prevent insulation performance deterioration due to condensation and freezing of humid ambient air. Second, the maximum temperature of the cryogenic insulation must not exceed 100°C during the booster re-entry. The resulting total insulation thickness was reduced by introducing a purge gap between the

cryogenic and the high-temperature insulation layer, through which pre-heated, dry gas shall be fed during the pre-flight tank filling phase.

An integrated test object of the insulation system including the purging system was build to thermally verify the insulation concept in the DLR test facility INDUTHERM. Both the steady-state tank refueling case with active purge flow and the re-entry case with the corresponding heat load acting onto the test object were successfully simulated. During the steady-state experiments, inlet gas temperatures ranging from 17°C to 38°C and inlet mass flow rates between 1.0g/s and 2.5g/s were tested for the purge flow and demonstrated the ability to control the temperatures within the system by varying those flow parameters independently in an achievable range with regard to future demonstration vehicles. Concerning the re-entry condition, the thermal protection system effectively shielded high temperatures from the underlying insulation layer.

In summary, the critical function of the temperature control by the integrated concept of cryogenic insulation, purge gap and TPS insulation was successfully verified. Due to the limited size of the integrated test object, further investigations regarding the gas management system, e.g. the gas supply system, the required inlet gas pressure and mass flow rates for an operational vehicle are necessary. However, a purge gap comes with an inevitable high system complexity, hence further investigations are recommended concerning the basic assumption of the first requirement regarding condensation and icing within the high-temperature insulation and its actual impact on the insulation performance.

References

[1] Cosson, E., Deneu, F., Coulds, O. L., Peypoudat, V., and Baiocco, P., "Thermal Architecture of Hydrogen Tank on RLV Second Stage," *4th European Workshop "Hot Structures and Thermal Protection Systems for Space Vehicles"*, Palermo, Italy, 2002.

[2] Johnson, T., Waters, W., Singer, T., and Haftka, R., "Thermal-Structural Optimization of Integrated Cryogenic Propellant Tank Concepts for a Reusable Launch Vehicle," *45th AIAA/ASME/ASCE/AHS/ASC Structures, Structural Dynamics & Materials Conference*, American Institute of Aeronautics and Astronautics, 2004. https://doi.org/10.2514/6.2004-1931.

[3] Sippel, M., Stappert, S., Wilken, J., Darkow, N., Cain, S., Krause, S., Reimer, T., Rauh, C., Stefaniak, D., Beerhorst, M., Thiele, T., Kronen, R., Briese, L. E., Acquatella, P., Schnepper, K., and Riccius, J., "Focused research on RLV-technologies: the DLR project AKIRA," *8TH EUROPEAN CONFERENCE FOR AERONAUTICS AND SPACE SCIENCES (EUCASS) 2019*, EUCASS association, Madrid, Spain, 2019. https://doi.org/10.13009/EUCASS2019-385.

[4] Sippel, M., Valluchi, C., Bussler, L., Kopp, A., Garbers, N., Stappert, S., Krummen, S., and Wilken, J., "SpaceLiner Concept as Catalyst for Advanced Hypersonic Vehicles Research," *7TH EUROPEAN CONFERENCE FOR AERONAUTICS AND SPACE SCIENCES (EUCASS) 2017*, EUCASS association, Milan, Italy, 2017.

[5] *ANSYS® Workbench Release 19.2.0*, ANSYS Inc., July 2018.

[6] Krummen, S., and Sippel, M., "Effects of the rotational vehicle dynamics on the ascent flight trajectory of the SpaceLiner concept," *CEAS Space Journal*, Vol. 11, 2019, pp. 161–172. https://doi.org/10.1007/s12567-018-0223-7.

[7] Evonik Resource Efficiency GmbH, "Rohacell® WF Product Information," , January 2019.

[8] Rath Group, "https://www.rath-group.com/produkte/hochtemperaturwolle/altrar," , August 2021.

[9] Reimer, T., Rauh, C., and Sippel, M., "Interface Designs between TPS and Cryogenic Propellant Tank of an RLV Booster Stage," *8TH EUROPEAN CONFERENCE FOR AERONAUTICS AND SPACE SCIENCES (EUCASS) 2019*, EUCASS association, Madrid, Spain, 2019. https://doi.org/10.13009/EUCASS2019-345.

[10] Baltex UK, "https://www.baltex.co.uk/spacerfabrics/," , July 2021.

[11] *ANSYS® CFX Release 19.2.0*, ANSYS Inc., July 2018.

[12] Rauh, C., Reimer, T., and Sippel, M., "Investigation of an RLV Cryogenic Tank Insulation Including a Purge Gap System," *International Conference on Flight vehicles, Aerothermodynamics and Re-entry Missions and Engineering (FAR) 2019*, Monopoli, Italy, 2019.

[13] Ferguson, P. W., Leonard, B. G., and Staszak, P. R., "Comparison of Integrated Cryogenic Tankage/TPS concepts for RLV Applications," *Space Technology Conference & Exposition, 1999*, Albuquerque, NM, USA, 1999.

[14] Poteet, C. C., Abu-Khajeel, H., and Hsu, S.-Y., "Preliminary Thermal-Mechanical Sizing of a Metallic Thermal Protection System," *Journal of Spacecraft and Rockets*, Vol. 41, 2004, pp. 173–182. https://doi.org/10.2514/1.9174.

[15] Johnson, T. F., Waters, W. A., Singer, T. N., and Haftka, R. T., "Thermal-Structural Optimization of Integrated Cryogenic Propellant Tank Concepts for a Reusable Launch Vehicle," *45th AIAA/ASME/ASCE/AHS/ASC Structures, Structural Dynamics & Materials Conference, 19-22 April 2004*, Palm Springs, CA, USA, 2004.